[redacted]

ACL AUTO-CONTROL LABORATORIES INC.

OS ANGELES AND PALO ALTO, CALIFORNIA

GPO PRICE $ _____

CSFTI PRICE(S) $ _____

Hard copy (HC) _____

Microfiche (MF) _____

ff 653 July 65

HIGH TEMPERATURE THERMOCOUPLE

RESEARCH AND DEVELOPMENT PROGRAM

APPENDIX 3

MISCELLANEOUS TECHNICAL DATA

To

SUMMARY REPORT NO. T-1097

Contract Number NAS 8-5438

Request Number TP 3-83547

Prepared For

GEORGE C. MARSHALL SPACE FLIGHT CENTER

Huntsville, Alabama

Work Performed By

AUTO CONTROL LABORATORIES, INC.

5251 West Imperial Highway

Los Angeles 45, California

Date of Publication 18 June 1965

Prepared By: R. R. Smith, Jr.

R. R. Smith, Jr.

APPENDIX 3

MISCELLANEOUS TECHNICAL DATA

INDEX

APPENDIX 3

LIST OF TABLES

APPENDIX 3

LIST OF ILLUSTRATIONS

APPENDIX 3

MISCELLANEOUS TECHNICAL DATA

1.0 GENERAL

This appendix incorporates all remaining technical data, other than drawings and calibrations.

2.0 HIGH MELTING POINT MATERIALS

A general survey of high melting point materials, from 3000°F to 6800°F has been made, and is presented in Table No. 2-1. This table has been compiled as a quick reference aid for future research.

2.1 Properties of Refractory Materials

As stated in numerous papers, the accumulated knowledge concerning the properties of refractory materials is in a state of constant change. The most comprehensive tabulation of characteristics found by ACL during this program was incorporated in a recent paper*. ACL obtained permission from the authors to reproduce Tables 2-2 through 2-7 from this paper.

*Updating the Refractory Materials, Machine Design, October 22, 1964, E.G. Kendall, Head, Metallurgy and Ceramics, and J.D. McClelland, Head, Applied Physics, Materials Sciences Laboratory, Aerospace Corp., El Segundo, California.

TABLE 2-1

HIGH MELTING-POINT MATERIALS*

Materials	Melting Point, °F	Materials	Melting Point, °F
Niobium carbide (NbC)	6800	Molybdenum carbide (Mo_2C)	4650
Graphite (C)	6700	Zircon ($ZrSiO_4$)	4622
Zirconium carbide (ZrC)	6400	Beryllium oxide (BeO)	4568
Tungsten (W)	6098	Cerium sulphide (CeS)	4440
Titanium nitride (TiN)	5800	Strontium oxide (SrO)	4406
Barium phosphide (Ba_3P_2)	5790	Silicon oxide (SiO)	4406
Titanium carbide (TiC)	5700	Yttrium oxide (Y_2O_3)	4380
Tantalum (Ta)	5440	Niobium (Nb)	4380
Zirconium nitride (ZrN)	5400	Columbium (Cb)	4370
Vanadium carbide (VC)	5090	Vanadium nitride (VN)	4280
Strontium zirconate ($SrO.ZrO_2$)	5070	Calcium zirconate (Ca.ZrO2)	4230
Magnesium oxide (MgO)	5070	Chromium oxide (Cr_2O_3)	4127
Zirconium oxide (ZrO_2)	4900	Zirconium silicides (Zr_3Si_2, Zr_4Si_3, Zr_6Si_5)	4010-4080
Molybdenum (Mo)	4760	Aluminum nitride (AlN)	4060
Barium zirconate ($BaO.ZrO_2$)	4748	Silicon carbide (SiC)	4000
Cerium oxide (CeO_2)	4712	Barium sulphide (BaS)	4000
Calcium oxide (CaO)	4660	Beryllium nitride (Be_3N_4)	4000
Barium nitride (Ba_3N_2)	3990	Barium oxide (BaO)	3490

TABLE 2-1

(Continued)

Materials	Melting Point, °F	Materials	Melting Point, °F
Chromium aluminide (CrAl)	3920	Beryllium oxide-aluminum oxide ($BeO.Al_2O_3$)	3470
Molybdenum aluminide (Mo_3Al)	3900	Silicon nitride (Si_3N_4)	3452
Spinel ($MgAl_2O_4$)	3874	Chromium carbide (Cr_3C_2)	3440
Titanium dioxide (TiO_2)	3866	Chromium (Cr)	3430
Calcium silicate ($2CaO.SiO_2$)	3866	Zirconium (Zr)	3350
Titanium silicide (Ti_5Si_3)	3848	Molybdenum beryllide ($MoBe_2$)	3344
Beryllium carbide (Be_2C)	3812	Mullite ($3Al_2O_3.2SiO_2$)	3290
Aluminum oxide (Al_2O_3)	3722	Zirconium beryllide ($ZrBe_9$)	3180
Niobium nitride (NbN)	3722	Vanadium (V)	3150
Molybdenum disilicide ($MoSi_2$)	3686	Silicon dioxide (SiO_2)	3110
Nickel oxide-aluminum oxide ($NiO.Al_2O_3$)	3668	Vanadium disilicide (VSi_2)	3020-3180
Beryllium silicate ($2BeO.SiO_2$)	3630	Molybdenum aluminide (MoAl)	3090
Barium oxide-aluminum oxide ($BaO.Al_2O_3$)	3630	Titanium (Ti)	3074
Magnesium sulphide-strontium sulphide (MgS, Srs)	3600	Nickel aluminide (NiAl)	3000
Nickel oxide (NiO)	3560	Zirconium aluminide ($ZrAl_2$)	3000
Niobium disilicide ($NbSi_2$)	3542	Zirconium disilicide ($ZrSi_2$)	3092

*Partially taken from: Missile Design & Development, April 1958

TABLE 2-2

PROPERTIES OF COMMERCIAL CARBIDES

Carbide	Melting Point (°C)	Thermal Conductivity (cal, cm/sec/deg C)	Coefficient of Thermal Expansion (in. in./deg C × 10⁻⁶)	Electrical Resistivity (ohm-cm × 10⁶)	Knoop Hardness kg/mm²	Modulus of Rupture (10³ psi)	Modulus of Elasticity (10⁶ psi)	Tensile Strength (10³ psi)	Compressive Strength (10³ psi)
HfC	3900	0.053(25)* 0.093(1900)	6.6(25-612)	37-65(20) 75-85(2200)	2500	34(25) 25(1090) 16(1310)	46(25)	...	...
TaC	3900	0.053(25) 0.077(2200)	5.5(20-2200)	30-41(20) 158(3200)	1800	31(25) 17.5(2000)	41(25)	30-35(25)	...
CbC	3500	0.034(25) 0.089(1900)	6.2(20-1900)	35-74(20)	2400	35(25) 3(2000)	49(20)	...	...
ZrC	3400	0.049(25) 0.112(2200)	9.1(20-2000)	42-67(20) 136(980)	2600	30(25) 4.5(1750) 2.5(2000)	69(25) 51(1000)	28(25) 13(1000)	238(25)
TiC	2940–3250	0.041(25) 0.110(2000)	10.2(20-2000)	60(20) 110(800) 125(1000)	3200	124(25) 13.5(2000)	45(25)	68(25) 18(1000) 9(1200)	109(25)
SiC	2700	0.099(25) 0.040(1540)	5.9(20-2000)	10^2-10^5(20)	2500	36(25) 27(1090) 31(1370) 21(1400) 13(1480)	68(25) 49(1500)	25(25)	150(25)
B_4C	2450	0.065(25) 0.20(425)	4.5(20-800)	0.3-0.8(25)	2880	50(25) 23(1425)	65(25)	44(25) 22(980)	414(25)

*All numbers in parentheses indicate temperature, C

TABLE 2-3

PROPERTIES OF COMMERCIAL GRAPHITES

Graphite	Thermal Conductivity (cal/cm-sec-deg C)		Coefficient of Thermal Expansion (in./in.-deg C)		Electrical Resistivity (μ ohm-cm)		Modulus of Elasticity (10^6 psi)		Compressive Strength (10^3 psi)		Flexural Strength (10^3 psi)	
	wg*	ag*	wg	ag	wg	ag	wg	ag	wg	ag	wg	ag
ATJ Nat'l Carbon	0.27	0.27	2.2	3.4	1200	1400	1.40	1.15	8.3	8.5	3.3	3.3
RVA, Nat'l Carbon	0.26	0.22	1.6	2.8	1200	1600	1.84	1.30	10	9	3.8	3.0
ATZ, Nat'l carbon	0.35	0.20	0.6	8.5	700	2300	2.89	0.73	8.9	11.4	5.9	2.3
CFZ, Nat'l Carbon	0.31	0.31	2.0	2.5	1100	1300	1.87	1.55	10.0	11.0	3.8	3.2
HLM-85, Great Lakes	...	...	2.2	3.4	700	1000	1.5	...	7.2	7.0	3.5	2.7
MHLM-85, Great Lakes	...	...	2.8	2.7	...	800	1.5	1.5	6.0	5.8	3.0	3.6
3499, Speer	0.24	...	3.2	4.4	450	...	0.8	...	6.0	6.5	3.6	..
8882, Speer	...	...	3.8	5.0	350	...	...	...	7.8	8.5	3.3	3.0
890 T, Speer	...	...	2.0	3.9	240	...	...	...	6.5	...	3.7	..
AHDJ, Am. Metal	0.24	...	1.7	1.4	800	900	1.30	...	10	...	3.7	..
PG	0.4-1.0	0.005-0.008	0.5-1.7	7.5-22.0	200-500	2.5-8×10^5	3.75	...	14	50-82	23	..

*wg = with grain; ag = against grain.

TABLE 2-4

CONVERSION FACTORS FOR HIGH-TEMPERATURE PROPERTIES OF GRAPHITES

	500 C	1000 C	1500 C	2000 C	2500 C
Coefficient of thermal expansion	1.50	1.75	2.00	2.25	2.50
Thermal conductivity	0.60	0.40	0.30	0.25	0.22
Electrical resistivity	0.75	1.00	1.30	1.40	1.50
Modulus of elasticity	1.05	1.15	1.25	1.35	...
Compressive strength	1.1	1.2	1.3	1.5	...
Flexural strength	1.1	1.2	1.4	1.5	2.2

TABLE 2-5

PROPERTIES OF REFRACTORY OXIDES

Oxide	Melting Point (°C)	Specific Heat (cal/g)	Thermal Conductivity (cal/cm/sec/deg C)	Coefficient of Thermal Expansion (in./in./deg C × 10⁶)	Electrical Resistivity (ohm-cm)	Hardness Moh's	Modulus of Elasticity (10^6 psi)	Tensile Strength (10^3 psi)	Compressive Strength (10^3 psi)
Alumina			0.084(RT)*				53(RT)	37(RT)	420(RT)
		0.19(RT)	0.023(500)	7.5(500)	10^{13}(500)	9	50(600)	33(1050)	210(600)
	2040	0.28(500)	0.014(1000)	8.5(1000)	10^{7}(1000)		45(1000)	18(1200)	120(1000)
		0.30(1000)	0.014(1500)	9.5(1500)			39(1200)	4(1400)	84(1200)
		0.32(1500)			10^{3}(1500)		29(1400)		35(1400)
									7(1600)
Beryllia	2550	0.24(RT)	0.52(RT)	8(500)	10^{9}(500)		43(RT)	15(RT)	170(RT)
		0.44(500)	0.15(500)	9(1000)	10^{7}(1000)	9	42(600)	13(700)	63(800)
		0.50(900)	0.050(1000)	10(1500)	10^{5}(1500)		32(1000)	10(1000)	35(1000)
			0.037(1500)				18(1200)	3(1200)	28(1200)
									24(1400)
									7(1600)
Magnesia	2950	0.24(RT)	0.095(RT)	12(500)	10^{12}(500)		30.5(RT)	14(RT)	...
		0.30(500)	0.034(500)	13.5(1000)	10^{7}(1000)	6	21.0	16(800)	
			0.016(1000)	15.5(1500)			10	10(1000)	
			0.014(1500)				4	8(1200)	
Thoria	3270	0.065(RT)	0.034(RT)	8(500)	10^{8}(500)	7	34(RT)	14(RT)	210(RT)
		0.075(500)	0.014(500)	9(1000)	10^{4}(1000)		31(600)		84(600)
		0.085(1000)	0.005(1000)	10(1500)	10^{2}(1500)		30(900)		50(1000)
			0.005(1500)						28(1200)
									5.6(1400)
									1.4(1500)
Zirconia	2850	0.13(RT)	0.004(RT)	8.5(500)	10^{7}(500)	7	24(RT)	21(RT)	290(RT)
		0.15(500)	0.005(1500)	9.5(1000)	10^{5}(1000)		16(1050)	13(1200)	170(1000)
		0.16(1000)		10.5(1500)	10^{2}(1500)		13(1360)	1.8(1500)	110(1200)
									18(1400)

*All numbers in parentheses indicate temperature, C.

TABLE 2-6

PROPERTIES OF REFRACTORY BORIDES

Boride	Melting Point (°C)	Thermal Conductivity (cal/cm/sec/deg C)	Coefficient of Thermal Expansion (in./in./deg C × 10⁶)	Electrical Resistivity (ohm-cm × 10⁶)	Knoop Hardness (kg/mm^2)	Modulus of Rupture (10^3 psi)	Modulus of Elasticity (10^6 psi)	Compressive Strength (10^3 psi)
HfB_2	3250	0.138(1600)*	5.5(25-1000)	12(25)	...	...	...	...
		0.310(2000)						
TaB_2	3100	0.276(260)	5.72(25-2200)	68(25)	4K$_{100}$	...	37(25)	...
		0.103(2200)			2530(25)			
ZrB_2	3060	0.104(260)	7.5(25-1350)	9-16(25)	4K$_{200}$	29(25)	50(25)	230(25)
		0.060(1920)			1915(25)			29(25)
								(Tensile)
CbB_2	3000	0.040(25)	...	32(25)	4K$_{200}$	...	29-44(25)	...
		0.047-0.062(200)			1820(25)			
					1260(900)			
TiB_2	2980	0.141(50)		10-30(25)	4K$_{100}$	35(25-2000)	60(25)	97(20)
		0.107(1000)	6.4(25-1250)	60(1000)	3370(25)			
					860(900)			
SiB_6	1950	...		0.2(25)	1950-2400(25)	...	...	...
			6.3(25-980)	0.1(970)				

*All numbers in parentheses indicate temperature, C.

TABLE 2-7

PROPERTIES OF REFRACTORY BERYLLIDES

Beryllide	Melting Point (C)	Thermal Conductivity (cal/cm/sec/deg)	Coefficient of Thermal Expansion (in./in./deg C × 10⁶)	Electrical Resistivity (ohm-cm × 10⁶)	Vickers Hardness (2½ kg @ 25 C)	Modulus of Rupture (10³ psi)	Modulus of Elasticity (10⁶ psi)	Compressive Strength (10³ psi)	Oxidation (mils/100 hr)
$CbBe_{12}$	1690	0.072 (760)*	5.20	55.5(25)	500	22(25)	47(25)	200(25)	0.9(1370)
				166.6(650)		45(1260)	40(870)	130(870)	2.0(1480)
		0.078 (1480))		200.0(1260)		40(1370)	25(1370)	80(1370)	
						22(1510)	10(1510)		
Cb_2Be_{17}	1705	0.78 (760)	4.91	...	1000	31(25)	43(25)	15(25)	0.6(1370)
		0.082 (1480)				35(870)	40(870)	38(1260)	1.9(1480)
						70(1260)	25(1370)	28(1370)	
						63(1370)		18(1510)	
						36(1510)		(Tensile)	
								data)	
Cb_2Be_{19}	1705	...	...	...	1050	30(25)	...	...	...
						30(870)			
						70(1260)			
						65(1370)			
						27(1510)			
$TaBe_{12}$	1850	0.073 (760)	4.68	43.5(25)	720	31(25)	45(25)	150(25)	0.5(1370)
				111.1(650)		53(1260)	40(870)	190(870)	0.9(1480)
		0.090 (1480)		117.6(1260)		43(1370)	20(1370)		
						26(1510)	10(1510)		
Ta_2Be_{17}	1985	0.071 (760)	4.85	...	1120	30(25)	45(25)	...	0.3(1370)
		0.078 (1480)				40(870)	40(870)		0.9(1480)
						78(1260)	20(1370)		
						56(1370)	10(1510)		
						35(1510)			
$ZrBe_{13}$	1925	0.087 (760)	5.48	16.1(25)	1000	25(25)	47(25)	190(25)	0.5(1370)
				76.9(650)		40(1260)	40(870)	150(870)	1.3(1480)
		0.087 (1480)		100.0(1260)		37(1370)	20(1370)	70(1370)	
						25(1510)	10(1510)		
Zr_2Be_{17}	1980	...	4.66	...	1130	25(25)	45(25)	...	0.5(1370)
						40(1260)	40(870)		1.2(1480)
						40(1370)	20(1370)		
						35(1510)			
$MoBe_{12}$	1650	0.076 (870)	...	...	950	42(1260)	15(870)	...	0.3(1370)
		0.072 (1425)				30(1370)	12(1370)		0.6(1480)
						13(1510)	1(1510)		
$H_{12}Be_{21}$	>1925	...	5.03	...	...	20(1260)	28(870)	...	...
						24(1370)	15(1370)		
						17(1510)	10(1510)		

*All numbers in parentheses indicate temperature C.

3.0 FABRICATION OF TUNGSTEN

3.1 Cold Working

One of the most persistent problems encountered in fabricating gauges made from vapor deposited Tungsten is in preventing development of work strains in the material during grinding and cutting operations.

The reasons for concern are related to the cause of failure in previously tested samples. Failures examined under a microscope exhibited very large grain growth, similar to that seen in sintered, recrystallized Tungsten. To understand the mechanics of such failures under dynamic and static loading, it is necessary to realize the physical differences in the grain structure of the two types of material, although both are body centered in basic structure.

3.2 Sintered Tungsten

These materials are intensively worked both during the sintering process, and during the drawing process. This is particularly true of tubing. Microscopic examination of etched samples reveals the formation of extremely large grains, associated with embrittlement, and low strength. Such material is not suited to use in thermocouple gauges where the assembly is to be subjected to vibration, shock, and thermo-aerodynamic loading during use. Failures are sudden and invariably castrophic, as would be seen in glass.

3.3 Vapor Deposited Tungsten

This material, in its as-deposited form, because of the relatively small grain size, and very high purity, approaches a monolithic physical construction, with the attendant advantages of high strength, and practically no tendency to nucleization for the growth of large grains.

3.4 Embrittlement

Although the literature is very sparse on grain growth in the vapor deposited material, sufficient test data have been taken to form a basis for some conclusions as to desirable procedures. These conclusions may be set up as basic rules for working the material. It had been noted, in early attempts to utilize the material in high temperature structures, that there seemed to be a tendency toward development of embrittlement with heat, after the first temperature cycle. This condition was analogous to that condition seen in Tungsten wire (.040 - .125) which typically shatters under stress after recrystallization at about 2100°F. This characteristic has been noted in the vapor deposited material, but can also be related to the extent and nature of any cold working prior to use.

A solution to the problem was approached, assuming that the resistance to massive grain growth could be maintained, if nuclei for such grain growth could be avoided during cold working and surface finishing.

A series of 40 tubes, designed for long-term continuous use in a

3.4 Embrittlement (Cont'd.)

reactor (1600°C, 500 hours) were fabricated, with tolerances held as close as possible. Working was confined to light surface grinding, with final forming done with chemical milling. Of these 40 parts, only one failure was noted. The cause of this failure is not yet known, but there is good cause to believe the finishing process used is critical, and if controlled is successful in preventing large grain formation. Obviously, the most desirable process would eliminate the need for either grinding, or any other kind of cold working. At this time, this can be achieved only with very careful attention to design of the forming mandrels, and some sacrifice of surface appearance in the finished parts.

4.0 MATERIALS TEST

Because of concern with the strength and ductility of the sheath material used in the Type 4735 gages, an attempt was made to ascertain several characteristics over the temperature range from ambient to the brittle-to-ductile transition temperature. It is well established that Tungsten is a brittle material at normal temperatures. A general consensus seemed to be that vapor deposited Tungsten did not develop ductility at any temperature, and that vapor deposited Tungsten tubing exhibited little or no room temperature strength. ACL has long been convinced that this is not true because of the shock and vibration tests run very early in this project. A serious concern has existed, however, as to whether the

4.0 MATERIALS TEST (Cont'd.)

sheath materials could be surface finished without serious loss of strength, at room temperatures.

The brittle-to-ductile transition temperature has been established as approximately 400°C.

Four Tungsten tubes, each 3/8 inch long, .250 inch inside diameter, and .030 wall thichness were prepared for the test. Two of the tubes were surface ground on a belt-sander to remove the rough, as-received surface. Approximately .005 inch of material was removed in the grinding. The specimens were then placed horizontally between the platens of a compression tester and loaded radially until failure occurred. Failure was defined as occurring when the tube collapsed. Table 4-1 below, shows the results of this test.

Table 4-1

COMPRESSION TEST

Sample Surface Character	Pounds Loading at Failure
Ground	150
Unground	95
Ground	140
Unground	105

4.0 MATERIALS TEST (Cont'd.)

One of the points of concern had been that grinding would provide a detrimental condition, in that it would create small surface marks that might aggravate the known notch-sensitivity of the Tungsten. The results of the test indicate that surface grinding actually improved the strength of the material, under the conditions of test, by about 50%. The nature of the fractures in the material at failure support the argument that the grinding removed very sharply defined microscopic peaks and valleys in the surface of the material, thus eliminating incipient points of failure due to stress concentration. The unground specimens both broke axially, with long cleavages. The ground specimens suffered a nearly explosive type of fracture with very small pieces resulting from the fracture, and developed no well-defined pattern of cleavage. It would appear, then, that grinding the surface permits higher loading by permitting the locked-in stresses to build to a higher value, with cleavage along a random pattern of grain boundaries when the stresses are relieved at failure.

5.0 FORMING MANDRELS

The mandrels used to form the first generation sheaths were made in two pieces. Difficulty was encountered in withdrawing the two-piece mandrels from the sheaths because of adherence between the Tungsten and mild steel of the mandrel. It was necessary, therefore, to etch the steel out with concentrated hydrochloric acid. Although this method works, it is time-

5.0 FORMING MANDRELS (Cont'd.)

consuming and introduces the possibility that a small piece of steel may be left in the tip, near the junction. The present mandrels are one-piece construction. Although the formation appears somewhat more difficult, there is a net saving in time, and the probability of successful mandrel withdrawal is increased. A simple qualitative test then is used to determine whether all steel has been removed. If necessary, any remaining steel can be etched out. Should any steel remain in the sheath, it will liquify with increase in temperature, and, since Tungsten is soluble in molten steel, a failure could result.

6.0 POST MORTEM EXAMINATION, TYPE 4734 GAUGES

The two Type 4734 gauges previously tested at N.A.S.A. in a scale rocket engine were disassembled and examined.

6.1 Gauge Serial No. 003

This probe was run at 10 diameters downstream of the rocket nozzle. An open circuit was observed after 3 seconds. The examination of the part quickly revealed that the junction had been melted away, thus explaining the open circuit. The probe was completely disassembled, and the piece parts were examined.

The sheath was found to be severely eroded for about two inches from the deflection shield used for mounting, although the front portion was

6.1 Gauge Serial No. 003 (Cont'd.)

relatively undamaged except for the tip itself.

It is believed that the steel of the deflection shield flowed back up the sheath upon melting. Tungsten, being soluble in molten steel, went into solution as the steel flowed forward. Boundary layer theory of laminar separation would seem to support this belief*.

Internally, the brazed joint between the copper conductor and the Tungsten sheath remained intact, as did the brazed joint between the Tungsten Rhenium center conductor and its cupro-nickel lead wire. In the region of the copper joint, the Beryllium oxide was intact, although it had melted near the tip. Ateflon seal at the back end of the body of the gauge was undamaged. The stainless steel of the body was undamaged. All screw-joint parts functioned normally.

6.2 Gauge Serial No. 001

This probe was run at 40 diameters for 15 seconds, shut down and reinstalled at 20 diameters, then run for 10 seconds.

Upon receipt of the gauge the sheath was broken at a point just inside the mounting fitting. The break was typical of the type of break previously induced in the 4734 sheaths by a sharp-edged blow, or excessive shock. The broken faces of the sheath show evidence of oxidation, which

*High Speed Aerodynamics, Hilton, Longmans Green & Co., P.P. 587-588

6.2 Gauge Serial No. 001 (Cont'd.)

indicates the break occurred during or prior to the run.

The junction was found to be intact, as well as all other electrical connections.

7.0 FORM AND DRAG

7.1 Discussion

The attitude of the gauge relative to flow is important to the designer, when the performance objectives of life, response, resistance to oxidation, erosion, shock, vibration, and loads caused by immersion in the flow are considered.

There are essentially three conditions of attitude relative to flow to be considered:

a. With the gauge mounted transverse to flow, and with flow impingement normal to the longitudinal centerline of the gauge.

b. With the gauge mounted such that flow is parallel to the longitudinal centerline of the gauge, with the medium impinging on its tip.

c. With the gauge mounted such that the flow is turbulent, stagnated, or with unpredictable flow vectors.

7.2 Transverse or Parallel Mounting

If the gauges were mounted in a medium with a well-established and defined flow pattern, it follows that attainment of the different design objectives would be affected as described in the following paragraphs.

7.3 Mounting Considerations

If the gauge is mounted either transverse to flow, or parallel to flow, response to a step-function change of temperature will be inversely related to the mass velocity seen in the region of the junction. Response is also a function of the mass of the tip structure and the junction, as well as the diffusivity of the materials, Thus, the most favorable conditions for fast response are those of high velocity, low mass in the gauge tip, and good thermal transfer characteristics of the materials. If, conversely, the gauge is mounted in a region where there is no flow, or very low flow, response is predicated upon the mass of the junction and its structure, and the thermal characteristics of the materials. Thus, the designer is on the horns of a dilemma if he is faced with the requirement of designing a probe to satisfy both general requirements: i.e. no flow, and high mass velocity. In addition, he is further faced with another dilemma, in that he can not extend the life of the gauge by employing a structure of high mass in a high mass velocity flow, if he is to meet the fast response requirement in a no-flow condition. A low-mass structure, with fast response under no-flow, simply does not lend itself to immersion in a high mass velocity medium because of the

7.3 Mounting Considerations (Cont'd.)

accelerated effects of erosion and oxidation.

There is, additionally, the requirement of resistance to the effects of vibration and shock to be considered. The desirable structure would have a small cantilever, with decreasing mass from the base to the tip, a natural frequency of the basic structure outside the vibration spectrum to be encountered, and high internal damping.

For resistance to bending and shear forces developed during exposure to high velocity flows, the immersed portion of the gauge should have a geometry which incorporates low drag characteristics over a wide range of mach numbers, from subsonic to supersonic. Since the local velocity of sound in a given medium is related only to temperature, a preliminary investigation of the mach numbers likely to be encountered was made, and is presented later. Suggested cross-sectional shapes suitable for immersion in the flow are the double wedge, single wedge, and biconvex.

7.4 No-Flow Considerations

It is apparent that the response of the gauge will have to meet certain minimum requirements. Under no-flow, or unpredictably turbulent conditions, designing for fast response presents an entirely different set of problems.

7.5 The Free-Standing Shape in a Flow

It is felt, at this stage of the program, that the geometry or the immersed portion of the probe will very heavily influence the internal design features because of physical spacing available. Therefore, a preliminary investigation of free-standing shapes for the flow field was started. Results of this investigation are given below.

7.6 Mach Numbers in the Flow

The $\frac{Cp}{Cv}$ of the medium is not presently known. Moreover, it is not known how $\frac{Cp}{Cv}$ will vary, with time and temperature. Therefore, values of M were calculated for $\frac{Cp}{Cv}$ from 1.0 to 1.5, Absolute Temperatures from 773°C to 3273°C, and local velocities of 1000 to 5000 feet per second.

Local speed of sound was calculated with the following relationship; which gives exact values.

$$a^2 = \gamma RT$$

Where:

a = local speed of sound, feet per second

γ = ratio of specific heats, $\frac{Cp}{Cv}$ dimensionless

R = universal gas constant, dimensionless

T_A = temperature, °C absolute

Mach numbers for M = V/a at discrete values of T, and V were then calculated, and the data plotted as a complex graph, (See Figure 7-1) from which could be taken the local Mach number for any combination of

7.6 Mach Numbers in the Flow (Cont'd.)

parameters given above. It is seen, from the graph of Figure 7-1, that if the extremes of conditions within the total envelope of the values selected for calculation were encountered, the local Mach number could vary from M = 3.25 at γ = 1.0, V = 5000 ft/sec and T_A = 773°C to M = .25 at γ = 1.5, V = 1000 ft/sec, and T_A = 3273°C.

It is realized that such wide variations will not be seen under actual stabilized flow conditions. However, it is expected that actual Mach numbers will fall within the calculated envelope. It is seen, moreover, that fluctuations in any parameter can shift the Mach number by a considerable amount, and that resolution of the operational profile must be accomplished before a final selection of the geometry of the free-standing member can be made, and a minimum - drag, maximum strength probe for accomodation of all parameters will be extremely unlikely, if not impossible. It is possible, however, to hypothesize a probe cross-section to operate within the envelope, which would exemplify desirable characteristics in a widely fluctuating flow field.

7.7 The Hypothetical Probe

a. General

It will be assumed, in this discussion, that:

1.) Maximum temperature = 3000°C

2.) Maximum velocity = 5000 ft/sec

3.) $\frac{Cp}{Cv}$ = 1.4 (approximately)

7.7 The Hypothetical Probe (Cont'd.)

This set of parameters yields a Mach regime from about M = .9 to M = 1.5 as the absolute temperature changes from about 1273°C to 3273°C.

Since the flow may be expected, then, to fluctuate from subsonic to supersonic, the character of the reaction of a member immersed in both subsonic and super sonic flow must be considered. First, the nature of the mathematical equations used to estimate coefficients of process will change from elliptical at subsonic flow, to parabolic at supersonic flow, which changes the $(M^2 - 1)$ 1/2 term of such equations from imaginary to real. This represents a fundamental change in flow pattern, which says that, at supersonic velocities, no warning of the presence of a solid body is transmitted ahead of the body.

It can be shown that, in accordance with Ackeret's first order theory, drag and increase of drag with incidence retain the same sign as at subsonic speeds. However, the angle of minimum drag, which is zero on Ackeret theory, now has a second order Busemann term and changes in sign when going supersonic.

7.8 Supersonic Flow

It can be further shown that the single or double wedge is a desirable cross sectional shape for immersion in a supersonic flow, when minimum drag is a primary consideration, although such a shape, examined under

7.8 Supersonic Flow (Cont'd.)

two-dimensional theory, exhibits undesirable lift characteristics. Since design requirements need not be concerned with lift, a shape exhibiting low drag and poor lift under both subsonic and supersonic flow is indicated. A properly designed wedge or double wedge may satisfy these conditions.

7.9 Double Wedge (Rhombus)

It is assumed for purposes of discussion that streamlines in the flow can be represented with a set of parallel, equidistant lines. These lines will be deviated until they are parallel to the entering surfaces of the rhombus by the attached shock. The flow continues parallel to each surface until it arrives at the beginning of the expansion around the point of maximum thickness. As the flow goes through the expansion, it is swung around the corner, increasing speed and decreasing pressure until the Mach angle in the faster flow on the rear surface is attained. The expansion then ceases, and the flow continues until the compression shock at the trailing edge is reached. The flow is then turned parallel with the original undisturbed streamlines. This process obtains for both sides of the rhombus, and the flow from both sides joins without discontinuity. This does not mean, however, that forces cancel and zero drag results. To the contrary, the radiation of pressure waves requires energy, and shows up as wave drag.

7.10 Single Wedge

The general arguments applicable to the symmetrical double wedge apply as well to the single wedge, under first order Ackeret theory. In the case where a bluff trailing edge is employed in the single wedge, a friction wake develops. The absolute pressure over the bluff base can not be calculated because of breakaway of flow, but it has been measured. These values have been used, then, in calculating drag coefficients for various thickness to chord (t/c) ratios which indicate that the single wedge offers an advantage over the double wedge for ratios over 12%. Ratios of absolute base pressure to free stream static pressure in the order of 1/3 have been measured in wind tunnel tests at Mach numbers near 1.5. It can also be shown that, even with a vacuum on the base of a single wedge, the critical ratio is only 20%, above which a considerable advantage in reduction of drag, as compared with the double wedge, is realized.

A sketch showing pictorially the various conditions discussed above, is presented in Figure 7-2.

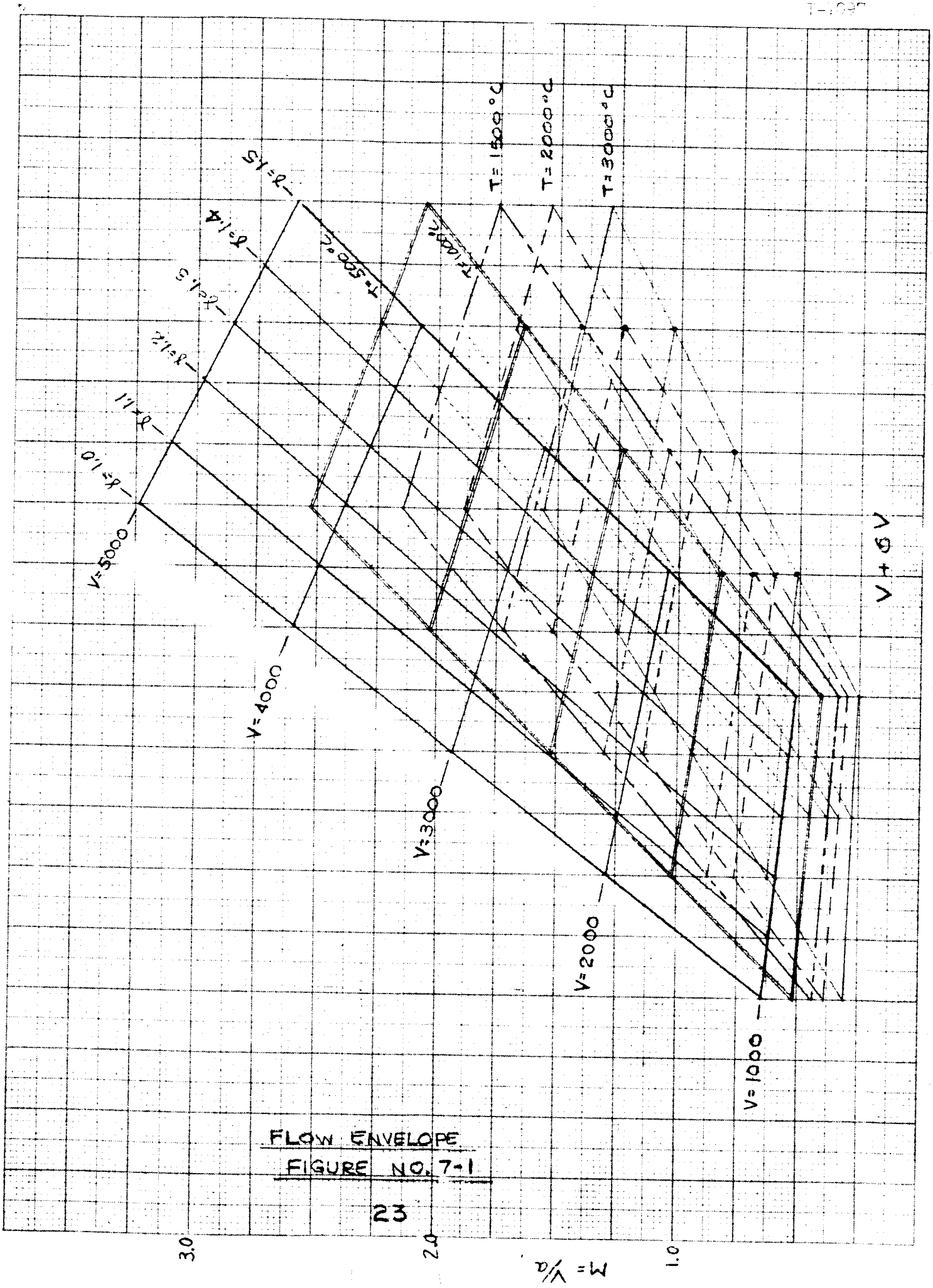

FLOW ENVELOPE
FIGURE NO. 7-1

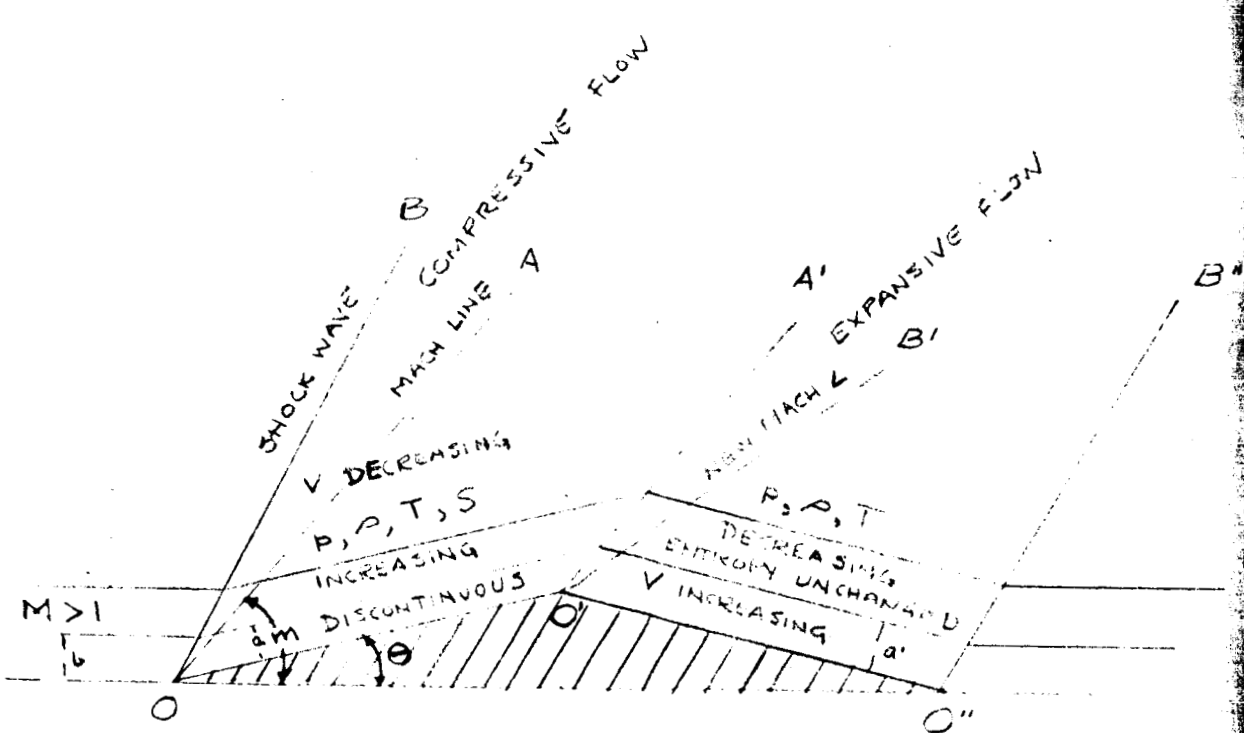

RHOMBUS IN SUPERSONIC FLOW

FIGURE NO. 7-2

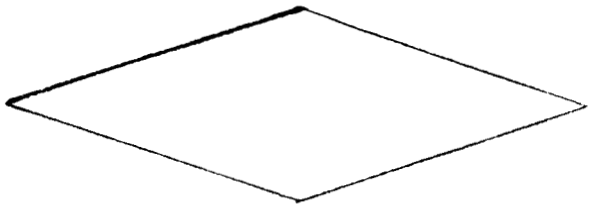

DOUBLE WEDGE (RHOMBUS)

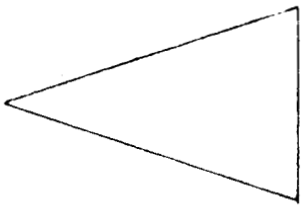

SINGLE WEDGE

BICONVEX

POSSIBLE TWO-DIMENSIONAL SHAPES

FIGURE NO. 7-3

7.11 Analysis, Aerodynamic Loading

All information, regarding the medium in which the gauges will run, has not been received. Therefore, a definitive analysis is not possible. A general assessment can be made, however, of the effects of aerodynamic loading, in arbitrary terms. The general geometry of the Type 4735 prototype gauges was used in preparing the estimates of form drag and shock drag shown in Figures 7-3 and 7-4, respectively.

7.12 Form Drag

The form drag was calculated for a projected area of 2.36×10^{-3} ft.^{2}, medium velocity to 5000 ft/sec, and medium densities of 2.045×10^{-3}, 2.37×10^{-3} and 3.567×10^{-3} slugs per ft.^{3}. The curves are shown in Figure 7-4, with maxima from 55 pounds to 95 pounds. An immersion depth of 1.8 inches was hypothesized. These curves take the usual shape associated with form drag. A drag coefficient of 0.9 was used in all computations. The loads thus indicated did not account for failures seen in tests of other gauges of similar type. Therefore it was suspected that a shock condition may have existed.

7.13 Shock Drag

To obtain an estimate of shock drag, a geometry similar to the Type 4735 gauge, but incorporating a Biconvex cross section with a t/c ratio of 37.5% was hypothesized, and it was assumed that the flow would to supersonic at some point in the temperature-velocity regime.

7.13 Shock Drag (Cont'd.)

The projected area was estimated at 1.547×10^{-3} ft.^{2} at 1.8 inches immersion depth. The ratio of specific heats of the medium at 1.3, and a value of 58 was given 2K. Density, taken at 0.56×10^{-3}, at ambient, was corrected for the discrete temperatures of 773°K, 1273°K, 2273°K and 3273°K, selected for the estimate. Velocities of 2000, 3000, 4000, and 5000 ft/sec were likewise used. Results of the computations were plotted, using a modified "carpet" technique, and are shown in Figure 7-5.

It is emphasized that, since values selected for the various parameters were not necessarily those to be actually encountered in use, no significance can be placed on any data point in the carpet. However, the graph does indicate that, depending upon the combination of temperature and velocity attained at light-off, and during the short time internal thereafter, until stability is reached, there is a possibility of an extremely large load "spike" occurring for a brief period of time, and a consequent catastrophic failure in the immersed member, if loaded transversely. The existance of such "spikes" in other tests has been suspected for some time. No other reasonable explanation has been advanced for random, dramatic failures of probes being tested in various engines and gas generators. Such failures have been invariably associated with fuel-rich starts and/or unstable burning. That events in the sequence of ignition and combustion happen in very short time intervals is well known; vis: the pressure rise of 250,000 psi/sec, and the

7.13 Shock Drag (Cont'd.)

suspected presence of a short duration, very high temperature spike in a current, large reaction motor.

The two estimates of dynamic loading given above are not based upon actual operating parameters. It is felt however, that the shock drag may present a problem worthy of consideration, if only because of the relative magnitude of the forces developed.

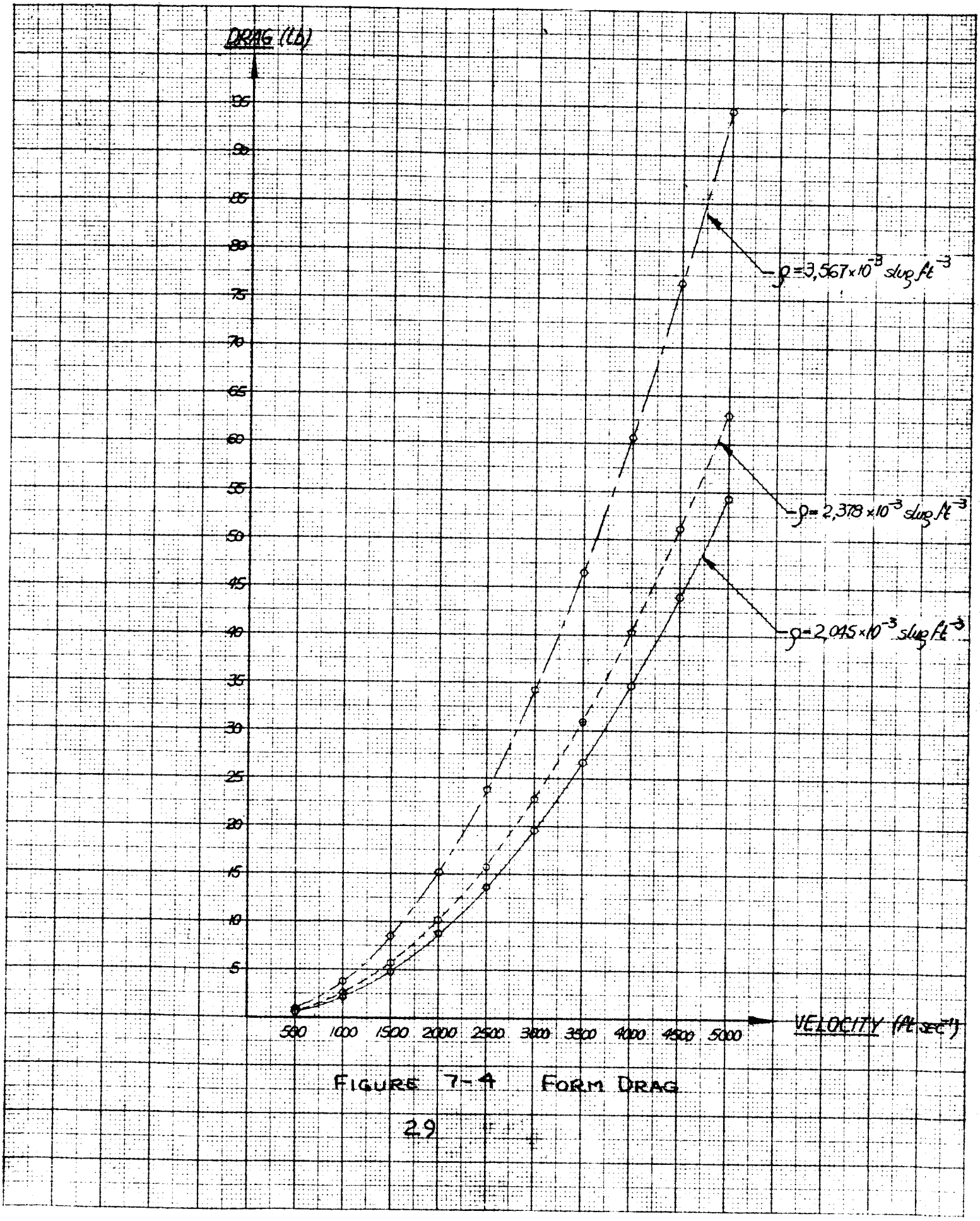

FIGURE 7-4 FORM DRAG

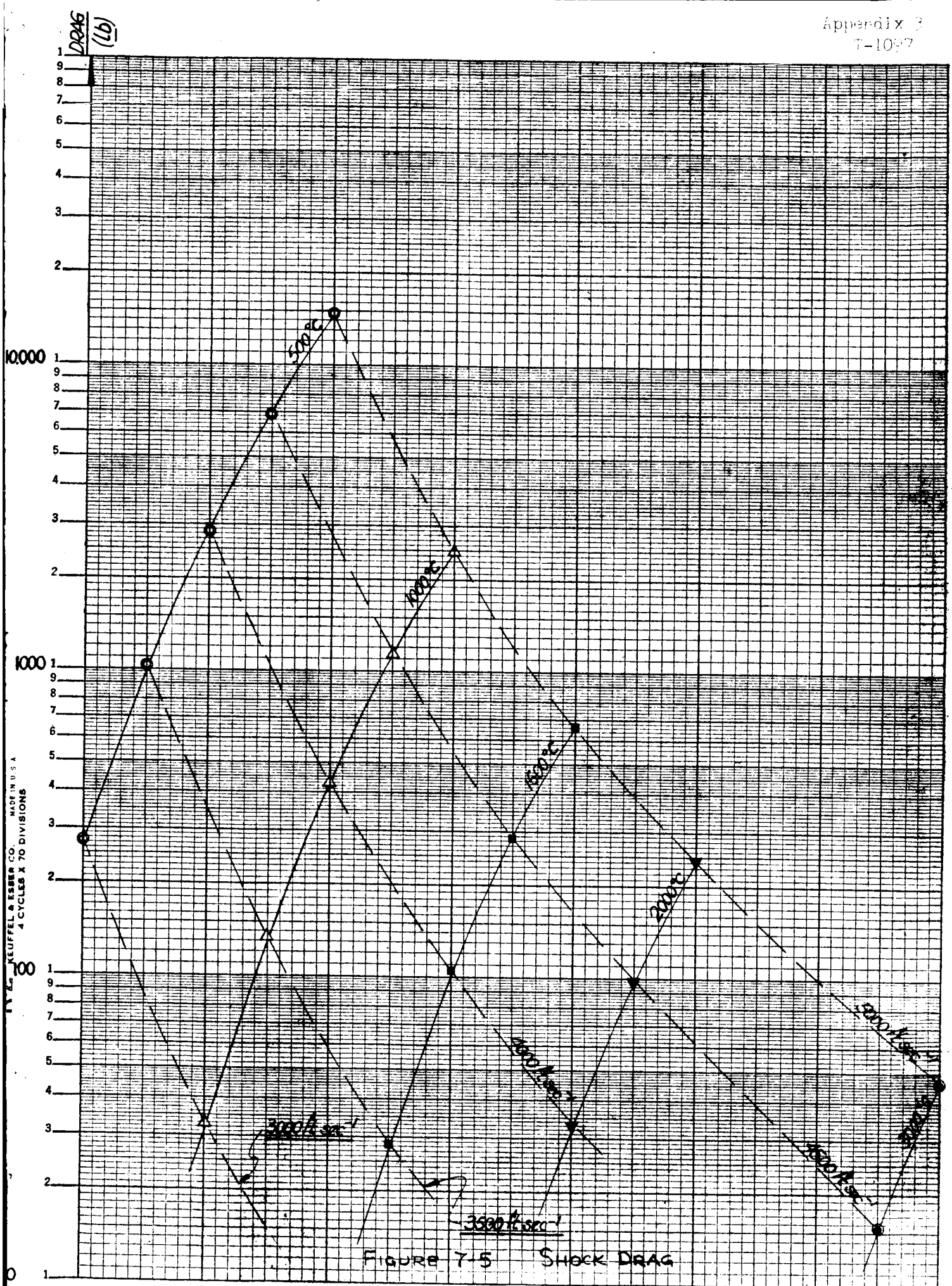

FIGURE 7-5 SHOCK DRAG

8.0 HIGH TEMPERATURE INSULATORS

8.1 Discussion

In searching for electrical insulation adequate for use at elevated temperatures it was found that ordinarily available literature contains little or no information regarding electrical characteristics at temperatures above approximately 1600°C (2912°F). Contact was established with Hughes Aircraft Company, Documentation Research Section, Culver City, California, which is engaged in Electro-Physical Properties of Matter research under a Government contract. A similar contact was established with Purdue University, Thermophysical Properties Research Center.

In parallel with the literature searches mentioned above, ACL compiled empirical data, as well as comparisons of existing published data concerning high temperature insulators. A comparison of values is tabulated below.

TABLE 8-1

OXIDE INSULATORS, PROPERTIES

Property	BeO Beryllia	Al_2O_3 Alumina	Zr_O2 Zirconia	MgO Magnesia	ThO_2 Thoria
Melting Point °F	4650	3700	4830	5070	5970
Hardness (Mohs)	9	9	6.5	6	6.5
Density gm/cc	3.0	3.97	6.1	3.6	9.7
Thermal Conductivity (Cal/Sec °C-cm^2/cm)					
100°C	.525	.072	.005	.086	.025
600°C	.112	.022	.005	.028	.010
1000°C	.049	.015	.006	.017	.007
Thermal Shock Res.	Excellent	Good	Fair	Fair	Fair
Electrical Resistivity (ohm/cm)					
100°C	--	1×10^{15}	1×10^{6}	--	--
600°C	--	2×10^{10}	8×10^{3}	--	1×10^{7}
1000°C	8×10^{12}	2×10^{7}	1×10^{2}	1×10^{13}	1×10^{5}
1200°C	3×10^{12}	2×10^{5}	--	8×10^{11}	2×10^{4}
1600°C	2×10^{10}	--	--	--	becomes conductor
2200°C	--	--	--	exp. upper* limit	--
2450°C	exp. upper limit*	--	--	--	--

An examination of Table 8-1 shows that Alumina is eliminated because of its low melting point, Thoria because of its poor thermal shock characteristics and low resistivity, Zirconia because of its low resistivity.

*Exact value not known

8.1 Discussion (Cont'd.)

Of the two materials remaining, Beryllia is clearly the better, because of its characteristic of remaining an electrical insulator to a higher temperature than Magnesia, even though the Magnesia has a higher melting point.

Another family of materials exhibiting high melting points, but concerning which little information was available electrically, is the Zirconates. Table 8-2, below, lists those with high temperature characteristics in the range of interest.

TABLE 8-2

ZIRCONATES*

Material	Melting Point °C
$BaZrO_2$	2700
$3BeO \cdot ZrO_2$	2345
$CaO \cdot ZrO_2$	2345
$MgO \cdot ZrO_2$	2120
$SrO \cdot ZrO_2$	2700
$ThO_2 \cdot ZrO_2$	2800
$ZrO_2 \cdot SiO_2$	2420

*Ref: High Temperature Technology, Wylie, N.Y., 1956, I.E. Campbell, Ed.

8.1 Discussion (Cont'd.)

Although it is obvious from Table 8-1 that Zirconium Oxide, which is common to all these compounds, is unsuitable as an insulator in its pure form, the degree to which the combination of compounds affects their electrical characteristics is not known. The basic measurement of resistivity over a wide temperature range is beyond the monetary scope of this project. However, it is felt a limited investigation should be performed to determine whether there may be grounds for future work on these materials. They should also be examined for possible use as protective materials.

8.2 Oxide Insulators

As evidenced in both the Southern Research Institute report and the ACL tests, if presently available electrical insulators are used in a high temperature probe, the upper operating temperature is limited by the characteristic behavior of the insulator. That is: the insulator becomes conductive at some elevated temperature.

There is wide disagreement between leading authorities as to the exact mechanism of the change in the ceramic from insulator to conductor. At present, the consensus is preponderantly in favor of Beryllia as the most effective of the oxides, and probably the best of the high temperature insulators. In meetings with research personnel at Los Alamos, the merits of Beryllia, Magnesia, Thoria, and Hafnia were thoroughly

8.2 Oxide Insulators (Cont'd.)

discussed. In their experience, an upper limit of 4200°F to 4500°F is attainable with Beryllia in applications of the type under consideration in this project. Other sources* report the presence of even small amounts of other materials effects a significant change in the phase change temperature of the internal structure of the material.

The maximum temperature of effective use, without degredation of insulation characteristic is greater by consensus, with Beryllia than with the other ceramics.

8.3 Base Insulation

Since base temperatures, although relatively high, are less than those to be seen at the tip of the gauge, an electrical insulator with the capability of remaining an electrical insulator at temperatures less than the maximum temperature at the tip, can be employed. A suitable insulator for this purpose is Magnesium Oxide (MgO). This material offers the following characteristics:

Melting Point - 4800 - 5070°F

Coef. Thermal Exp. @ 2200°F - Approximately 7.7 x 10^{-6}/°F

Density - 2.5 - 2.6 gm/cc

*Guide to Refractory Ceramics,
Materials in Design Engineering
Vol. 58, No. 1, PP 86 - 96
July 1963

RTD Technology Briefs,
Vol. 1, No. 10, PP 1 - 6, Oct. 1963
Hq, Research & Technology Division
Bolling AFB, Wash. 25, D. C.

8.3 Base Insulation (Cont'd.)

Resistivity - ohm/cm @ 2500°F - 10.5 x 10^3

Thermal Shock Res. - Fair

Hardness - 5 Mohs scale

It is planned to use this material in the finely divided form, and compact it mechanically to attain sufficient rigidity to prevent creation of voids in the base cavity. Use of the material in the powder form may also provide internal damping in an attempt to avoid vibration damage.

8.4 Gas Dielectrics

One area of approach had not been given serious attention until current evidence indicated that availability of a true high temperature insulator was unlikely within the time imposed by this contract. In investigating the electrical insulation characteristics of other materials, it was found that some materials, undergoing a change of state at 600° to 700°C, become a gas with very high dielectric strength. One such material is Sulfur Hexafluoride. It is recommended that these materials be more thoroughly investigated in future work.

8.5 No Insulation Approach

During a previous high temperature instrumentation program conducted by ACL, a Tungsten vs Tungsten-26% Rhenium thermocouple was used to measure temperatures in the order of 5000°F in an induction furnace. Good correlation was obtained between the predicted output curve for the

8.5 No Insulation Approach (Cont'd.)

present, are not appreciable enough to cause a deviation in output beyond ordinary limits of tolerance.

It was planned, therefore, to set up the test run at carefully controlled temperatures, with angularities from 180° to some lower limit determined by test. At the same time, the temperature at the junction of the test thermocouple was monitored with a calibrated standard probe.

The end objective was to fabricate a gauge incorporating no electrical insulation within the sheath.

In the early attempts to run the no-insulation tests, a gross error in concept invalidated the first runs. In these tests, the simulated thermocouple was located in an isothermal zone. No errors in output, as compared with a standard thermocouple probe were noted. At first inspection, no notice was taken of the validity of the setup itself. Upon re-examination it was apparent that no useful information could come from the setup as made. With the entire test block and the thermoelectric elements at the same temperature when the oven was stabilized, there would be no temperature differential existing at any point in the immersed portion of the system.

The major objective of the test was to find whether a probe could be constructed without electrical insulation such that current leakage

8.5 No Insulation Approach (Cont'd.)

between conductors of the pair in the absence of an insulator would not deteriorate the output from the junction to the extent that the probe would be rendered useless. With the system in an isothermal zone, and at equilibrium, all parts of the system would be at the same temperature with the exception of a small differential due to thermal conduction along the lead wires (which were of the same material as the thermocouple). If current leakage between the legs of the pair occurred, in the isothermal zone, the effect would be identical to that occurring in a set of thermocouples hooked up in parallel. That is, the net effect of the leakage would be to average the outputs of a large number of parallel junctions, all at the same temperature. Therefore, the setup was revised to include the effect of a suitable temperature differential.

8.6 No Insulation Test

The test setup used to perform "No-Insulation" Tests is shown in Figure 8-1.

8.6 No Insulation Test (Cont'd.)

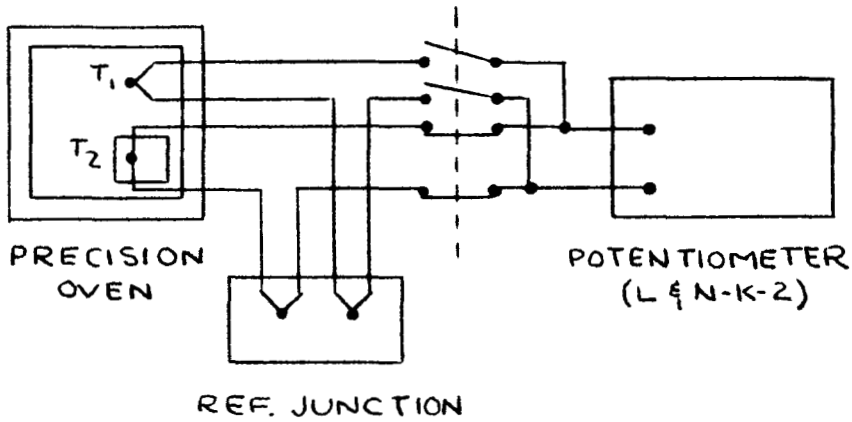

Figure 8-1

"No Insulation" Test Setup

The ceramic test block was provided with lines scribed in degrees, from 180° to 10° separation between conductors. Movable pins afforded means of changing angularity between the thermocouple pair of T_2. Thermocouple T_1 was a conventional premium grade insulated probe, calibrated against an NBS secondary standard. The reference junction temperature was 32°F (melting point of ice).

The measuring block was an L & N K-2 Potentiometer calibrated to N.B.S. standards. The test block is shown in Figure 8-2 below.

8.6 No Insulation Test (Cont'd.)

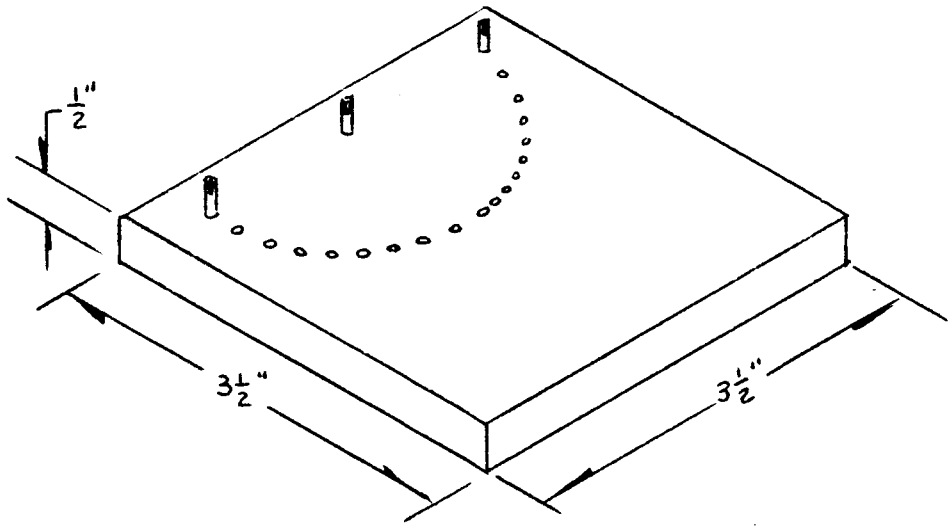

Figure 8-2

Test Block

There was no discernible difference in output (within .01 mv) between the reference thermocouple and the test block pair from 180° to 10° angularity. These results, however, were not conclusive, as the difference in outputs due to Thompson effect could be expected to increase as a function of the output, which would increase from 7.94 mv at 300°F to 50.05 mv at 1600°F.

9.0 VIBRATION TEST

9.1 Discussion

After a mock-up gauge had survived the 60 g, 11 millisecond shock test described in Appendix 3, Para. 10.0, the shock tests were suspended and the test fixture, with the mock-up mounted in the same manner, was set up on an electro-mechanical vibrator. The specimen was then subjected to a vibration scan from 10 to 2000 cps and from 2000 cps to 10 cps with a log sweep rate in 15 minutes. As in the shock test, only the Y-axis was investigated. From 10 - 30 cps, the displacement was .21 inch double amplitude, and up to 50 g from 20 - 2000 cps.

No resonance was revealed during this test, nor was there any evidence of physical damage.

9.2 Calculations

Calculation of the natural frequency of such a structure yielded results as follows:

Assumptions:

Modulus of elasticity - 6×10^7

Damping factor - 2.5

Density - 10.7 Oz/in^3

Length - 2.0 inches

Outside diameter .270, Inside diameter .250

9.2 Calculations (Cont'd.)

The exact dynamic method was chosen for the estimate:

$$f_n = \frac{(KL)^2}{2} \quad \frac{EIG}{WL^4}$$

f_n = natural frequency in cps

K = damping factor (assumed = 2.5)

L = Length, inches = 2.0

L^4 = 16 .

E = Modulus of elasticity = 6×10^7

$I = \frac{\pi r^4}{4} = .7854\ (.135)^4 = 4.91 \times 10^{-6}$

G = Acceleration of gravity, inches = 386

W = Weight, lbs., = .0117 lb.

$$f_n = \frac{(2.5 \cdot 2)}{2} \quad \frac{6 \times 10^7 \cdot 4.91 \times 10^{-6} \cdot 386}{1.17 \times 10^{-2} \quad 16} = 3100 \text{ cps}$$

Since the 2nd and 3rd natural frequencies are also far above the band-pass of the required frequency spectrum, they were not estimated.

9.3 Vibration Test

Vibration testing had been performed, prior to this test, on a mock-up of the Type 4735 Gauge. A completed gauge had not, however, been subjected to investigative tests to determine its response to sinusoidal vibratory inputs in the range 5 to 2000 cps.

The gauge tested had been temperature cycled repeatedly from ambient

9.3 Vibration Test (Cont'd.)

to more than 5000°F. Any effect of recrystallization on the physical structure of the sheath had, therefore, been fully realized. The principal concern in this regard was whether high temperature cycling would induce an early failure in the sheath material, since any gage calibrated to the temperatures of interest would have had every opportunity to recrystallize, and it is hardly likely that a virgin gage would be used in an application.

During the tests, both input to the fixture and output at the gage nut were monitored with calibrated accelerometers, over the frequency range and inputs shown in the data sheet of Figure 9-1. The gage was vibrated at each resonant frequency for two minutes. The resonances search was conducted over the range with a logarithmic sweep in 45 minutes.

The gage was examined following the test. No evidence of structural damage was seen. The gage function was unimpaired as a result of the test.

The input was held to 14 g at the resonances for two reasons: to permit measuring the Q of the gage, and to prevent extreme amplification at the resonant points. Table 9-1 below, lists resonant frequencies and the amplification factor for each.

9.3 Vibration Test (Cont'd.)

Table 9-1

AMPLIFICATION FACTOR "Q"

	Resonant Frequency cps	Input g	Output g	Amp. Factor Q
Z-Axis	125	14	24	1.7
	270	14	24	1.7
	450	14	50	3.6
	700	14	36	2.6
	1310	14	60	4.3
X-Axis	440	14	20	1.4
	560	14	50	3.6
Y-Axis	105	14	28	2.0
	155	14	28	1.6
	475	14	42	3.0
	510	14	47	3.4
	1125	14	44	3.1
	1400	14	58	4.1

The "Tube" referred to in the data sheet is the sheathed extension lead wire of about 18 inches in length, with a B-nut on the end. The reaction of this lead may have contributed to the relatively high response as seen above.

FORM L-6

AUTO-CONTROL LABORATORIES INC.

5251 West Imperial Hwy., Los Angeles 45, Calif., OR 8-4934
Northern California: 499 Hamilton Ave., Palo Alto, DA 1-4811

VIBRATION DATA SHEET

CUSTOMER A-C
PART THERMOCOUPLE
DESCRIPTION
PART NO. 47[illegible]-2
SERIAL NO. 0001
REF.

PAGE 1 OF 1
JOB NO. T-1097
DATE 4-13-[illegible]
SPEC.
TEST BY [illegible]
WITNESS [illegible]

AXIS	TEMPERATURE DEG. FAH.	RESONANCE SEARCH	RESONANT FREQUENCE (CPS)	FREQUENCY RANGE (CPS) FROM	FREQUENCY RANGE (CPS) TO	VIBRATION AT RESONANCE (MIN.)	VIBRATION CYCLING (HOURS)	ACCELERATION (G'S)	DISPLACEMENT (IN. P-P)
Z	Rm	Yes	—	5	14				0.1
			—	14	45			4.0	
			—	45	85				0.035
		Yes	—	85	2000			INPUT 14.0 OUTPUT —	
			125			2.0	TUBE		24.0
			270			2.0	TUBE & PROBE		24.0
			450			2.0	PROBE		50.0
			700			2.0	TUBE & PROBE		36.0
			1310			2.0	" "	14.0	60.0
X	Rm	Yes		As Shown	Above			As Shown Above In 1st Four Columns.	
			140			2.0	PROBE	INPUT 14.0 OUTPUT 20	
			560			2.0	TUBE	14.0 [illegible]	
Y	Rm	Yes	—	As Shown	Above			As Shown Above In 1st Four Columns.	
			185			2.0	TUBE	INPUT 14.0 OUTPUT 28.0	
			155			2.0	TUBE & PROBE		22.0
			475			2.0	PROBE		42.0
			510			2.0	TUBE		47.0
			1125			2.0	TUBE & PROBE		44.0
			1450			2.0	"	14.0	58.0

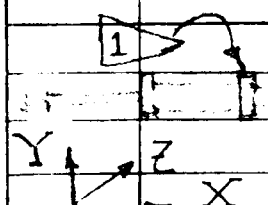

NOTES 1 → Out Put Accelerometer Was Mounted At This Point.

6

9.4 Type 4700 Gauges

Vibration testing had been performed on the Type 4735 gauges to limited (14g) input levels, as discussed previously. In order to more fully establish the characteristics of the sheath materials of the Type 4735 gauges within scope of work requirements, two additional tests were performed to sinusoidal input levels of 60 G, without failures, which exceeds the objective of 50 G by 10 G. The test articles, methods, and results are described below:

9.5 Test Articles

Two test sheaths, each of different construction, were fabricated of vapor deposited Tungsten, using the same techniques of construction as in the Type 4735 gauges. They are described separately as follows: as Gauge "A" and "B" for identification.

9.6 Gauge "A"

Gauge "A" was made with a biconvex cross section, 0.103 inch in the minor axis, and 0.258 inch in the major axis. Unsupported immersion length was 1.50 inches. (See Figure 9-2). The last inch of length from the tip was tapered 8-1/2°, in the major dimension and 1° in the minor dimension. Nominal wall thickness was .020 inch, although the wall thickness in the monor axis may have been as thin as 0.008 inch in places, because of variations in straightness prior to final dimensioning. The center conductor was W26Re, 0.020 inch in diameter, vapor deposited

9.6 Gauge "A" (Cont'd.)

in the tip to form a junction with the Tungsten sheath. It was unsupported over its length. This gauge had not been heated, therefore it was in the raw, or non-recrystallized condition.

9.7 Gauge "B"

Gauge "B" was made with a tubular, symmetrical cross section, 0.123 inch outside diameter, and a nominal 0.020 wall thickness. Unsupported immersion length was 1.95 inches. (See Figure 9-2). The last inch of length from the tip was tapered 1°. As in the Type "A" gauge, the 0.020 inch W26Re center conductor was vapor deposited in at the tip, and was unsupported over its length. This gauge had been temperature cycled from 2000°F to 4300°F at least six times, and was therefore fully recrystallized.

9.8 Test Method

The test gauges were cast in Devcon "B", a dense cement, with their unsupported immersion length extending from the cement block. The block was tightly clamped in a vibration fixture mounted on the head of a Ling electrodynamic vibrator. Calibrated accelerometers mounted on the head and the gauge base were used to measure input and output accelerations. Inputs were increased in steps of 5g to a maximum input of 60g, at the resonant points found during a logarithmic sweep resonance search.

9.9 Test Results Gauge "A"

During the scan on Gauge "A", resonances were observed as follows:

Table 9-2

RESONANT FREQUENCIES, 4700 GAUGE "A"

Axis	Resonant Freq. cps	G Input	Max. G Output
Minor (Y)	1496	5	150
Major (X)	1497	5 - 10	235
	1500	5 - 60	saturated
Major (X)	3268	5	260

Time at each G-input level at resonance was a minimum of 15 minutes. No adverse effects were noted during or after this test.

9.10 Test Results, Gauge "B"

During the scan on Gauge "B", one resonance at 550 cps was noted. The gauge was subjected to inputs of 5g to 60g at resonance in 5g increments, and was vibrated at the 60g level for 15 minutes. No adverse effects were noted during or after this test.

9.11 Discussion

As can be seen from the descriptions of the two test gauges given above, there is a considerable difference in physical characteristics

9.11 Discussion (Cont'd.)

between the Type 4735 gauges previously vibration tested, and Gauges "A" and "B". The fineness ratios of Gauges "A" and "B", however, are considerably larger than the Type 4735 gauge. Therefore, these tests represent worst case conditions and may be taken as a measure of the reaction of the Type 4735 gauge sheath to vibratory inputs greater than those stated in the scope of work.

The major consideration for the tests described herein, was the resolution of whether the sheath material, in the configuration used in ACL Series 4700 gauges, was suitable for use under a severe vibration environment. The question was further compounded by the fact that; 1) ordinary Tungsten has a well established recrystallization temperature characteristic which is associated with a serious decrease in ductility, and 2) in the cold (ambient temperature) state is notoriously brittle. The vibration tests at ambient temperature therefore were performed under adverse conditions. A great deal of concern has been expressed by N.A.S.A., as well as others, whether the sheath material would fail under vibration, and it was considered necessary by ACL to prove or disprove this contention.

As a consequence of these vibration tests, it is concluded that the sheath material, vapor deposited Tungsten, as fabricated by San Fernando Laboratories, Pacoima, California, to ACL design configurations, and

9.11 Discussion (Cont'd.)

processed by ACL, is suitable for applications such as the Type 4735 gauges.

ACL had considered, moreover, that alternate sheath types, such as the Type "A" and "B" sheaths, should be investigated in the interest of the scope of work regarding sheath configurations for minimum drag and highest resistance to bending and shear forces.

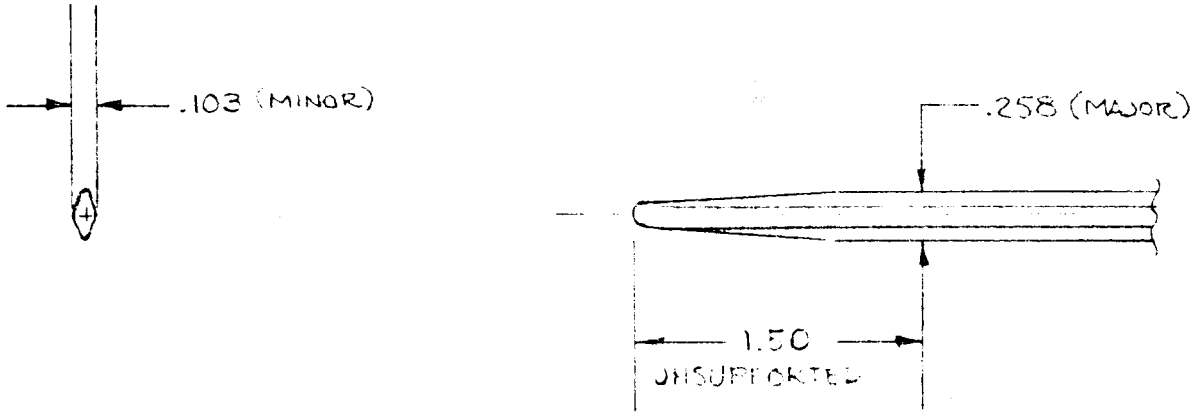

TEST GAGE "A"

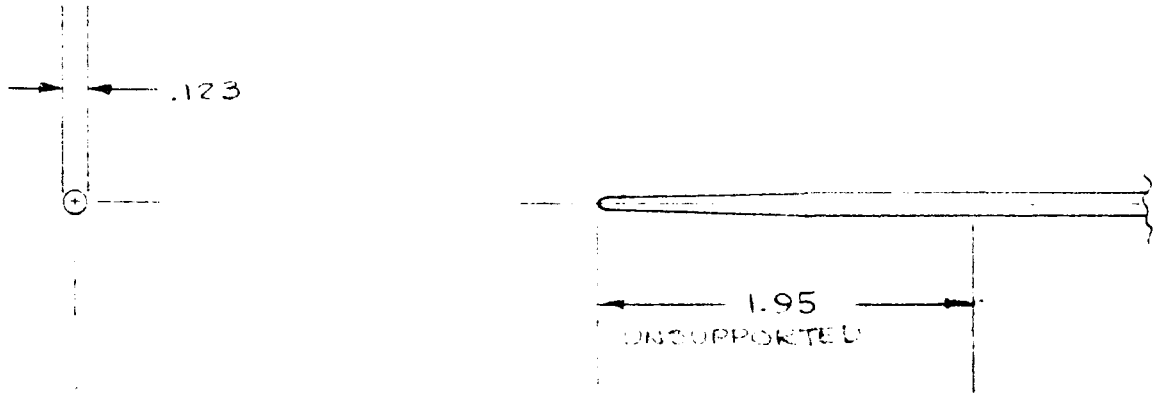

TEST GAGE "B"

FIG. 9-2 VIBRATION TEST GAGES

10.0 SHOCK TEST

10.1 Discussion

Reaction of the type of sheath, and the mounting used in the Type 4735 gauges to shock was a matter of concern, because of the generally brittle nature of refractory materials. Of primary concern was the sheath itself because of the scarcity of information regarding its tensile strength, and section modulus. A series of shock tests was therefore devised to investigate the ability of a mock-up Type 4735 sheath to withstand the shock requirement of this program.

Contract NAS 8-5438 states, under Article I - Scope of Work, Shock: 50 g's for a period of 6 to 11 milliseconds. The investigative shock tests were therefore, designed to approach these levels in controlled stages. It was decided to confine investigations at this time to the "worst" conditions; i.e. with the shock applied normal to the long axis of the immersed portion of the gauge, and with the cantilever of the sheath approximating the immersion depth selected for the first group of gauges. The sketch in Figure 10-1 below defines the axes of the test specimen.

The test specimen was mounted on a stainless steel tube, ground to the exact inside diameter of the specimen. Extension into the specimen was approximately .250 inch. This arrangement permitted mounting the specimen in an ACL Type 9335 compression fitting which was reamed to

10.1 Discussion (Cont'd.)

.290 I.D., for .020 inch clearance. The clearance space was filled with a chemically setting refractory cement.

A sketch of the specimen and fixture is shown in Figure 10-2. The shock tester, with specimen mounted, is shown in Figure 10-3.

For this particular shock test, the specimen was shocked only in the Y-axis, because the response of the gauge to the deceleration is most severe in this attitude, and represents the worst case for a cantilevered, symmetrical beam.

Since characteristics of the material were not well known, the severity of shock was applied in 10 g increments, at 11 milliseconds duration, starting with 10 g. Three shocks were applied at each level. After each shock, the specimen was inspected for evidence of damage. The test schedule is shown in Table no. 10-1.

It was originally intended that the specimen be tested to destruction. However, when the design objective of 50 g was exceeded, it was decided to investigate its response to vibration, in the interest of obtaining the greatest amount of information from an existing specimen.

10.1 Discussion (Cont'd.)

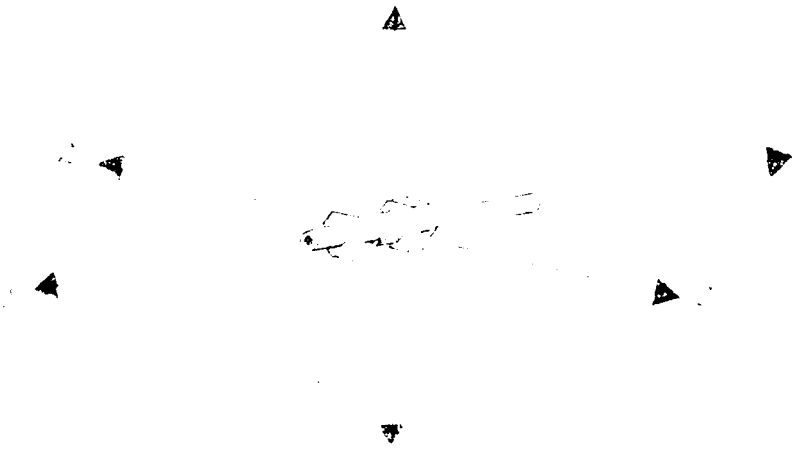

Figure 10-1

Definition of Axes

The mock-up was constructed as follows: A Tungsten tube, closed at one end and fabricated of the same material used in the 4735 gauges, was made with a length of 2.8 inches, inside diameter of .250 inch, and wall thickness of .020 inch.

This part approximates the type of sheath to be employed in the first prototypes, although there are significant differences in detail. The closed cylinder also offers the practical advantages of simplicity, availability, and lower cost.

10.1 Discussion (Cont'd.)

Table 10-1

SHOCK TEST SCHEDULE

g level	Duration	No. of Shocks
10	11 ms.	3
20		3
30		3
40		3
50		3
60	11 ms.	3

After imposition of shocks at 10 g, 20 g, 30 g, 40 g, 50 g, and 60 g, no damage was evident.

It is concluded, as a consequence of this test, that there is good evidence that a Tungsten tube, of the type tested, is capable of meeting the shock requirement of this project. This conclusion is further supported, when it is realized that the geometry of the prototype gauges will approach that of a constant strength beam, supported at one end.

BY ... DATE ... SUBJECT ... SHEET NO. ... OF ...
CHKD. BY ... DATE ... JOB NO. 17097

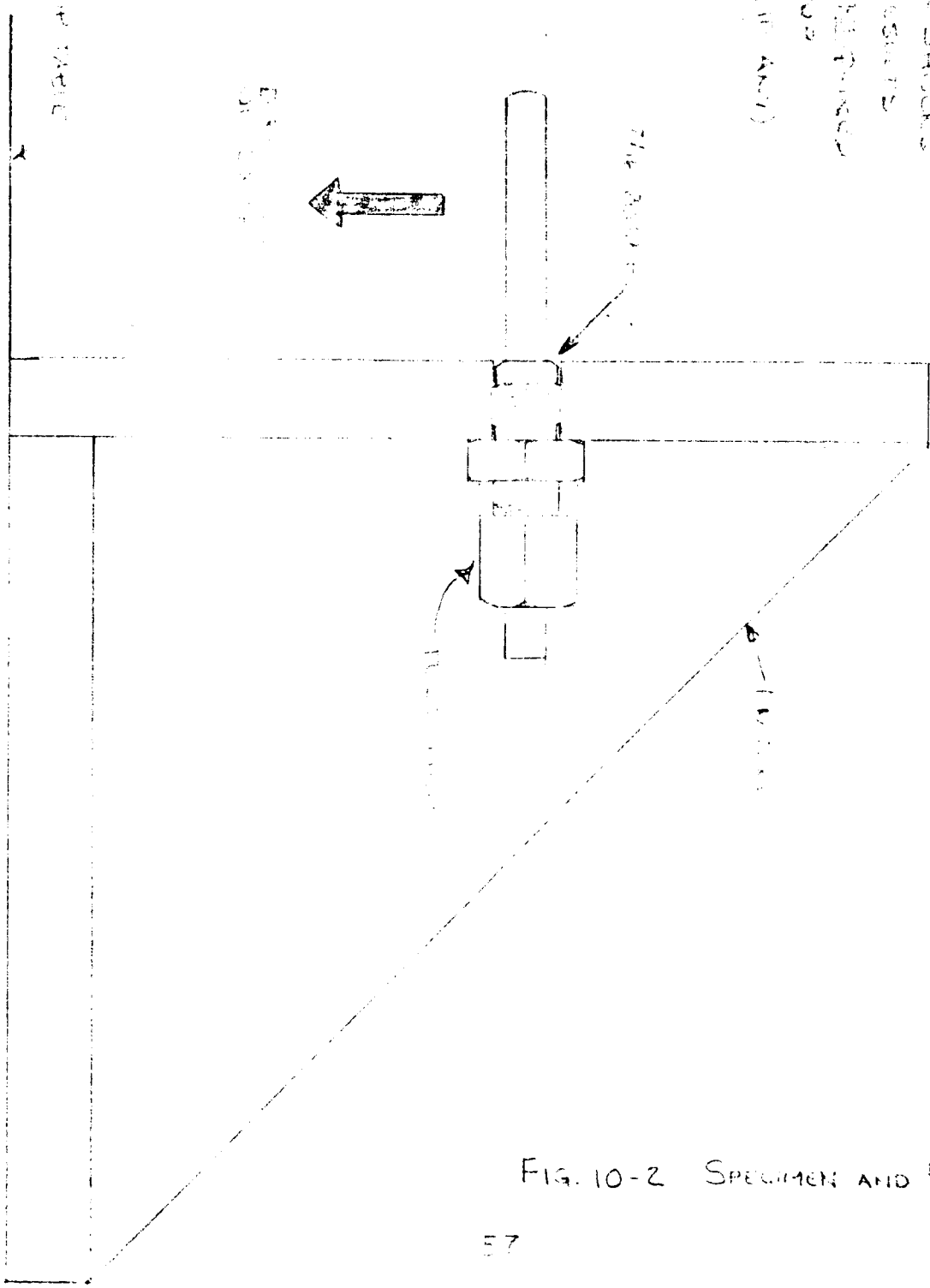

FIG. 10-2 SPECIMEN AND FIXTURE

ACL AUTO-CONTROL LABORATORIES INC.
5251 West Imperial Hwy., Los Angeles 45, Calif., OR 8-4934
Northern California: 499 Hamilton Ave., Palo Alto, DA 1-4811

11.0 PROTECTIVE COATINGS

11.1 Discussion

Protective coatings, as applicable to this program, are classified in two groups, oxidation resistant, and erosion resistant. Many such coatings have been developed over the past several years, and a great amount of data concerning their characteristics has been accumulated. Unfortunately, these data are extremely limited at temperatures above 3000°F. The secondary effects of the coatings upon the substrate is also an area in which little information is thus far available. The general thermal protective mechanisms upon which the coatings are based may be described as follows:

11.2 Ablation

The most common types of ablative coatings employ polymeric binders which undergo thermal decomposition to produce a firm porous carbon char, as well as gaseous by-products. The process is endothermic (heat absorbing), thus protecting the substrate against heat. The effectiveness of the process is measured by the amount of heat absorbed per unit weight of protective material used. This property varies, not only with the thermal conductivity of the material and the temperature, but also with other more subtle mechanisms working simultaneously.

11.3 Sublimation

As is seen in the definition of this latent process, subliming materials neither melt or decompose, but endure a change of state directly from the solid to the gaseous form. Large quantities of heat are thus absorbed until the subliming material is used up, at which time the protective mechanism ceases. Thus, if the heat of sublimation, the temperature and the quantity of the material, are known, the length of time for protection can be predicted.

11.4 Decomposition and Dehydration

When inorganic compounds decompose, appreciable amounts of heat are absorbed. Hydrated salts require large amounts of heat as the water molecules are forced out of the salts by the heat of hydration. Water molecules are forced out of the salts by the heat of hydration. Water itself is an outstanding example of a heat absorber as it changes from the liquid to the vapor state by the latent heat of vaporization.

11.5 Insulation

The efficient insulator protects from the effects of temperature by the introduction of a high thermal resistance (low thermal conductivity) between the substrate and the high temperature environment. Even the best available insulator, however, can not protect the substrate forever because of a finite thermal capacity in the substrate. An exception might be in the case where the substrate is capable of releasing the

11.5 Insulation (Cont'd.)

heat it is taken up by radiation, conduction, or convection, at a rate consistant with an acceptable temperature rise.

11.6 Intumescence

Intumescence occurs when a protective material swells and foams, upon exposure to high temperature, thus producing a small celled mass, whose coefficient of thermal conductivity is small. Additionally, the exposed surface chars to afford erosion resistance. These materials have measured characteristics as shown below in Table 11-1.

They are an interesting family of materials, and it is felt that a rather hard look should be taken at them for a possible application in this project.

11.7 Diffused Protective Coatings

The ACL Type 4734 gauges, produced under N.A.S.A. Contract NAS 8-4548, were provided with a diffused protective coating on the sheath. The materials in the coating were of two general groups: Disilicides, applied with a hot pack process (*Durak-B, Durak MG) and Silicon, applied by vapor deposition.

A large body of data, involving several thousands of hours of test, is available from Pratt and Whitney, Ling-Temco-Vought, Avco, and others,

*Chromalloy Corporation, Los Angeles, California

Table 11-1

INTUMESCENT COATINGS

Exposure Temperature	Medium	Coating Thickness	Heat Flux	Time	Material
2000°F - 3000°F	LOX-Fuel	.250 inch	Not Known	30 min.	Rigid Poly Urethane
**2000°F	LOX-Kerosene	.125 inch	Not Known		"
350°F - 6300°F	Not Known	.300 inch	1400 Btu/ft^2/sec	10 min.	Polymer
5000°F	Not Known	Approx. .020 inch	Not Known	60 sec.	Polymer
*2000°F - 3000°F	LOX-Kerosene	.090 - .125 inch		150 sec.	Urethane

The family of intumescent materials may incorporate several of the protective mechanisms described previously. Materials such as phenolics, ester resins, phenol-form, aldehydes, polyesters, silicones, and urethanes, may be used.

In addition to their flame resistant characteristics, these materials may also be compounded to resist the deleterious effects of various oxiders, such as N_2O_4, LOX, IRFNA and fuels such as Kerosene, UDMH, H_2.

*Saturn SA3 Test
**Atlas-Mercury Test

11.7 Diffused Protective Coatings (Cont'd.)

regarding the disilicides of Molybdenum and Tungsten, but only to temperatures in the order of 3000°F, in oxidizing media.

Early tests performed at N.A.S.A., Huntsville, on a few of the Type 4734 gauges, were productive, in that the gauges operated successfully, for short periods of time. Two of the gauges, thus tested, were transmitted to ACL on 25 July 1963, and were examined. In general, it can be said, on the basis of a first look, that the protective coatings held up quite well.

Tests previously performed at ACL, in a highly oxidizing medium at temperatures from ambient to approximately 4000°F revealed that the disilicide coating protected the gauges for a total of 19 minutes, during six cycles, and for 2 minutes at near 6000°F in a reducing medium for one cycle.

11.8 Protective Coatings, Research Summary

Early in this program, it was realized that a serious problem existed in retarding oxidation of Tungsten. At the time, the state-of-the-art was not well known. This area of endeavor, consequently, has received a great deal of attention. An extensive review of published literature has been made and the results of the search tabulated. (See Table 11-2) Only data that has been substantiated by test is reproduced in this table. Earlier tests at ACL of such materials, claimed by the manufacturer to have a protective quality at temperatures over 3000°F, were

11.8 Protective Coatings, Research Summary (Cont'd.)

disappointing in the extreme.

In researching the reports from which the data in Table 11-2 was taken, it became apparent that very little had been done toward taking data at temperatures above 4000°F, probably because the research programs were oriented toward long term oxidation resistance for structures at re-entry temperatures, rather than short term resistance for components, at high temperatures.

In other work reviewed, the degradation of silicide coatings at oxygen pressures from .1-76mm was studied by LMSC. In high velocity, low pressure air, a particular coating had a life of 2 hours, at 2700°F, but at one atmosphere, it lasted 15 hours. The failure mechanism appeared to be related to the evaporation of SiO under high temperature, low pressure conditions. The lowest oxygen pressure at which the SiO_2 film appears to be stable is 5mm O_2.

LMSC also investigated coatings for re-entry bodies at 3000°F to 4500°F. Their recommendation was for spray-coating of the W substrate with non-reactive oxides, using the oxide as a barrier to high velocity air, to reduce oxygen pressure at the substrate surface to a level such that oxidation rate is not a serious short term consideration. Tests of this technique at 3000°F and 5mm O_2 resulted in an increase in life in high velocity air from 8 minutes with uncoated Mo to 30 minutes with a

11.8 Protective Coatings, Research Summary (Cont'd.)

10 mil coating of ZrO_2.

Many researchers exhibited interest in a composite of refractory carbides and Tungsten. Typical of these is TaC-W. Aerojet-General reports that reaction between these two materials occurred after 2 minutes at 5400°F. General Telephone reported that eutectic formation occurs as low as 5160°F. Allison Division, G.M.C. reports the reaction temperature of W-TaC at 4980°F.

The consensus of the research groups seems to be that the coating exhibiting the most promising characteristics for short term use at temperature levels above 3000°F are modified disilicides, composites, and thin coatings of high refractory, non-reactive oxides.

11.9 High Temperature Reaction: Oxides, Nitrides and Carbides vs Tungsten

One of the tasks imposed in this contract is to investigate "the reaction of oxide coatings with Tungsten in relation to the emf output". This investigation has been in progress since the inception of the contract.

In comparing results obtained by various researches, Table 11-3 is presented incorporating data, not only regarding the oxides, but other materials as well.

11.8 Protective Coatings, Research Summary (Cont'd.)

Table 11-2

SUMMARY OF OXIDATION RESISTANT COATINGS

COATING	MFR	MIL THKNS	°F MAX TEMP	HRS LIFE	TESTED BY
Pt	AMF	5	3000	5	AMF
Diffusion (Undentified)	AMF	U U	2800 3200	10 3-4	AMF
W-2	Chromalloy	U	2700	60	Chromalloy
Si	G T & E	3-4	3300	0 -- 10	G T & E
Si-A	G T & E	3-4	3300	-- 10	G T & E
Si-B	G T & E	2	3300	-- 10	G T & E
Oxides (ZrO_2, ThO_2,BeO,HfO_2)	LMSC	10-30	3992	1 min. Failure by Oxidation	LMSC
Boron Nitride (Pyrolytic)	A.D.Little	U	3272	U	A.D.Little
Durak MGF	Chromizing Crop.	U	4600	10 min.	U
Ta-$HfO_2$50ThO_2	Harvey Aluminum	30	5000	U	U
Cr-ZrB	Value Engrg.	U	4000	35 min.	Redstone Arsenal
Silicide, Unmodified	G T & T	3	3272	11-16	G T & T
Silicide #1 Modified	G T & T	3	3272	19-26	G T & T
Silicide #2 Modified	G T & T	3	3272	20	G T & T
Sn-Al	G T & T	U	2000	8	
Binary Aluminide	Republic Aviation	U	3500	2.5	Republic Aviation

NOTE: U indicates unknown

11.9 High Temperature Reaction: Oxides, Nitrides and Carbides vs Tungsten

(Cont'd.)

The consensus seems to be that the refractory oxides, with the exception of MgO, are generally unreactive with Tungsten.

The refractory carbides and nitrides would be of little use as coatings on Tungsten at temperatures above the melting points of the eutectics, or at temperatures near those at which reaction was noted. It can thus be stated in general that above 5000°F the oxides are indicated but that some carbides and nitrides would be of use below 5000°F.

The tests were run on Tungsten foil which, having been mechanically worked, probably exhibits a grain structure much larger than the electrochemically formed sheaths of the Type 4735 gauges. Therefore, the interactions, particularly those associated with diffusion, may be quite different. The data, in Table 11-3, being essentially qualitative in nature, does not establish working ranges for the materials, but does serve as a basis upon which to predicate directed effort.

The effect of reactions of Tungsten with the oxides on the emf output of the gauge is not necessarily a straight forward function of temperature. From Table 11-3 it could be inferred that the non-reactive refractory oxides could be used with impunity to temperatures well above 5000°F. The effect however may occur in mechanisms other than those of chemical reaction. Used on the exterior of the gauge, Thoria, Zirconia,

11.9 High Temperature Reaction: Oxides, Nitrides and Carbides vs Tungsten

(Cont'd.)

Table 11-3

REACTION OF TUNGSTEN WITH OXIDES, NITRIDES AND CARBIDES AT ELEVATED TEMPERATURES

Material	Reaction
ThO_2	No reaction at 5430°F
ZrO_2	No reaction at 5430°F
BeO	Non reactive to 4200°F
MgO	Entirely reacted at 4530°F
UO_2	Not reactive at 5430°F
Al_2O_3	Vaporizing, but no other reaction at 5430°F
Y_2O_3	No reaction at 5430°F
HfO_2	Slight interdiffusion at 5240°F
TiN	Slight reaction at 5240°F
ZrN	Severe interface irregularities at 5430°F
TaC	W-TaC eutectic melted at 5160°F
HfC	W-HfC eutectic melts about 5070°F
ZrC	W-ZrC eutectic melts below 4890°F
(Ta-20Hf)C	W-(Ta-20Hf)C eutectic melts below 4890°F

The work resulting in most of the information in Table 11-3 was performed by General Telephone Electronics Labs. Others agree essentially with their results.

11.9 High Temperature Reaction: Oxides, Nitrides and Carbides vs Tungsten

(Cont'd.)

Yttria and Hafnia would not react. If they were not applied uniformly, however, the heating rate through the coating would be different and an error in output could result. If the coating thickness was too great, cracking and separation could occur, resulting in errors due to non-uniform radiative and conductive losses, as well as losses due to melting of the resultant oxides of Tungsten. Used internally, as electrical insulators, the oxides would perform like those used externally, except that there would be less effect of local increases of temperature due to stagnation of the medium. The greatest errors are more likely to occur because of the increase in electrical conductivity associated, in these materials, with high temperatures. Although there is some disagreement among researchers as to the changes in electrical conductivity, the consensus seems to be that the Zirconia, Hafnia and Yttria, although more refractory than Beryllia, become conductive at a lower temperature. Little information is available concerning Uranium Oxide in this regard.

11.10 Oxidation Tests

11.11 Preliminary Test

Concurrent with early calibrations a preliminary look at oxidation characteristics of the vapor deposited Tungsten was taken. A Tungsten slug was weighed before and after a run in air, at approximately 2200°F.

11.11 Preliminary Test (Cont'd.)

Weight of the slug prior to the run was 9.34 grams, after a two hour run, the weight increased to 9.61 grams; an increase of .27 grams, or 2.8%. Assuming the increase in weight is attributed to the formation of $W_2 O_3$, a loss of the parent metal to the formation of the oxide of about one gram per hour was experienced.

Since the oxidation rate can be expected to increase rapidly with temperature, and additionally with the percent O_2, a conclusion could not be drawn at that time, as to the rate of oxidation in use.

11.12 Oxidation Effects Type 4735 Gauge Serial No. 001, 3000°F

A recapitulation of oxidation tests, See Table 11-4, including a run to destruction, shows 4 hr. 37 min. running time up to 2000°F, 25 min. additional running time from 2000°F to 3000°F. See Figure 11-1.

The sheath material in the Serial No. 001 probe was elemental Tungsten, .030 inches wall thickness. No protective coating was employed. The mock-up used in vibration tests, fabricated of the same material, but with a wall thickness of .010 inch was then subjected to a run to destruction in the same test setup used with the 001 probe. A recap is presented in Table 11-5.

11.13 Oxidation Tests, 3000°F to 4500°F

One Type 4735 sheath assembly, previously used in lead wire calibrations, and response tests was subjected to oxidation tests within the temperature range of the calibrations. Following the calibrations, the gauge was run to destruction in an oxy-acetylene burner. After each cycle of running, the gauge was examined for evidence of deterioration. The thermocouple continued to operate to at least 4500°F. At 3000°F, the exposure was for 38 minutes. The temperature was then increased to about 4600°F, as observed with the optical pyrometer. After six minutes, the tip of the gauge oxidized away. Electrical insulation was not used in the tip of the probe during this test.

Microscopic examination of the probe tip showed the typical glassy material associated with Tungsten disilicide. Under these conditions, the siliconizing process apparently doubles the life of the probe, as compared with an uncoated probe.

11.12 Oxidation Effects Type 4735 Gauge Serial No. 001, 3000°F (Cont'd.)

Table 11-4

RUNNING TIME AT TEMPERATURE

Type 4735 Gauge, Serial Number 001

Run No.	Run Time Per Run Hrs.	Min.	Run Temp. °F	Total Run Time Hrs.	Min.	Remarks
1	1	10	1300°F to 2200°F	1	10	Atmosphere Argon Slight oxidation
1-1		30	1300°F to 2200°F	1	40	Argon Slight oxidation
2		30		2	10	Air, blue & purple oxides
3	2	27	1300°F to 2100°F	4	37	50% Argon, 50% Air, blue & purple oxides more pronounced
3-1		5	2768°F to 2984°F	4	42	Oxy-Acetylene Burner, yellow and green oxides started to form
3-2		7	3029°F to 3182°F	4	49	Yellow oxides more pronounced
3-3		6	2102°F to 3182°F	4	55	Yellow oxide formation, erosion apparent on 1st 1/2" of tip. Output good
3-4		5	2966°F to 3029°F	5	00	Yellow oxide formation, probe still functions.
3-5		2	2966°F to 3029°F	5	07	Heavy oxidation, output dropped off at 2 min. Probe failed.

11.12 Oxidation Effects Type 4735 Gauge Serial No. 001, 3000°F (Cont'd.)

Table 11-5

RUNNING TIME AT TEMPERATURE

MOCK-UP GAUGE

Run No.	Run Time Per Run Min.	Sec.	Run Temp °F	Total Run Time Min.	Sec.	Remarks
1	2	00	2500°F to 3000°F	2	00	Green and yellow oxides forming
2	4	00	2600°F to 3000°F	6	00	Heavy formation of green and yellow oxides
3	2	30	2600°F to 3000°F	8	30	Heavy yellow oxides formed, probe failed